Available online at www.sciencedirect.com
SCIENCE DIRECT®
Cement & Concrete Composites 26 (2004) 993–999
Cement & Concrete Composites
www.elsevier.com/locate/cemconcomp

Microstructural changes in concretes with sulfate exposure

Paul Brown [a,*], R.D. Hooton [b], Boyd Clark [c]

[a] Department of Materials Science and Engineering, The Pennsylvania State University, University Park, PA 16802, USA
[b] Department of Civil Engineering, The University of Toronto, Toronto, Canada
[c] The RJLee Group, 350 Hochburg Road, Monroeville, PA, USA

Abstract

In prior papers the responses of concretes to 50,000 ppm $MgSO_4$ exposure depending on cement type, w/cm and the presence of slag were described. The present paper completes this analysis by examining the effects of immersion of concretes produced using slag blended cements, in solutions containing 50,000 ppm of sodium sulfate. The spatial evolution of microstructure associated with carbonation and sulfate attack show differences which can be related to the nature of the cation associated with the sulfate, the cement type, and the w/cm ratio.

Keywords: Ettringite; Thaumasite; Cement type; w/cm Ratio

1. Introduction

Sulfate solutions are known to attack concrete and the most common ways to improve resistance to sulfate attack are (1) to reduce the permeability by restricting the water to cementitious materials ratio, and through use of supplementary cementing materials, and (2) to control the amount of reactive aluminate in the cement, typically by restricting the tricalcium aluminate content. The importance of permeability in controlling sulfate attack has been demonstrated for both laboratory and field concretes [1,2].

The nature of sulfate attack is well known to depend on the type of cations associated with the sulfate ions (e.g. [3]). Additionally, the cement type and presence of mineral admixtures have been shown to affect sulfate resistance. Prior work by Gollup and Taylor has evaluated the effects of sodium and magnesium sulfates on slag-containing cement pastes [4,5]. In the present study, these variables are examined with respect to the changes in microstructure which were produced after 21 or 23 years immersion of concretes in magnesium or sodium sulfate solutions, respectively.

2. Experimental program

Details of the experimental program were previously described [6,7]. In summary, concrete samples were prepared in April 1977 as control samples for a study on the sulfate resistance of slag cements. The ASTM Type V sulfate-resistant cement used contained 3.5% C_3A while the C_3A content of the ASTM Type II moderate-sulfate-resistant cement was 7.1%. The slag was from a Canadian source with an Al_2O_3 content of 8.52% and a Blaine fineness of 443 m^2/kg The concretes were air-entrained and 20 mm crushed glacial gravel of mixed siliceous and carbonate content was used as coarse aggregate. Further details regarding cement compositions and mix designs have been published elsewhere [8]. Concrete cylinders (75×150 mm) were cast at room temperature. Molds were stripped after 48 h and the concretes were stored in water at 23 °C until compressive strengths of between 29.7 and 33.1 MPa were attained. Subsequently, the cylinders were stored in 1000, 2000, or 3000 ppm SO_4 (as Na_2SO_4) solutions or in 3000 ppm SO_4 (as $MgSO_4$) solution. Various concrete properties were monitored every 3 months for 4 years. The concretes were then stored in a laboratory warehouse which was not air conditioned but was heated during winter, until an age of 8 years when they were visually inspected. At that time the sulfate exposure concentrations were increased to 50,000 ppm SO_4 (as Na_2SO_4) or

* Corresponding author. Tel.: +1-814-865-5352.
E-mail address: etx@psu.edu (P. Brown).

0958-9465/$ - see front matter © 2004 Elsevier Ltd. All rights reserved.
doi:10.1016/j.cemconcomp.2004.02.033

to 50,000 ppm SO_4 (as $MgSO_4$). Subsequent to this, they were again stored for three more years in the warehouse and then transferred to a 23 °C laboratory until they were obtained for the present study at an age of 21 years.

Samples were sliced from the cylinders using a diamond wheel saw in preparation for petrographic examination by SEM. Samples extended from perimeter surfaces inwards. These were then epoxy impregnated, polished, and carbon coated. SEM examinations and EDX analyses were carried out on polished sections.

3. Results and discussions

3.1. Type I cement + 45% slag, w/cm = 0.50, concrete exposed to 50,000 ppm of Na_2SO_4

The perimeter surface of this concrete was covered by a carbonated layer of variable thickness, ranging from about 50 to 100 micrometers, Fig. 1. Immediately beneath this layer is a region in which the microstructure is severely damaged. Networks of cracks radiate through the paste to a depth of about 6 mm in a manner typical of that observed as a result of sulfate attack [9], Fig. 2. Although cracks radiate from filled air voids, the paste is well bonded to the aggregate and to the slag granules. Evidence of a calcium hydroxide enriched interfacial zone is absent. As has been previously observed, the air voids near the surface are sometimes filled or partially filled with two sulfate-containing solids, ettringite and thaumasite. The distribution of these solids is shown in Figs. 3 and 4. Fig. 3 shows the microstructure and EDS spectra of thaumasite; Fig. 4 shows those for ettringite. Both spectra, however, show Si peaks indicative of an adjacent Si-containing solid. Other air voids are filled with thaumasite only, Fig. 5, while the paste porosity is predominantly ettringite filled, Fig. 6. This distribution of sulfate-containing solids is consistent with deleterious expansion being associated with the formation of

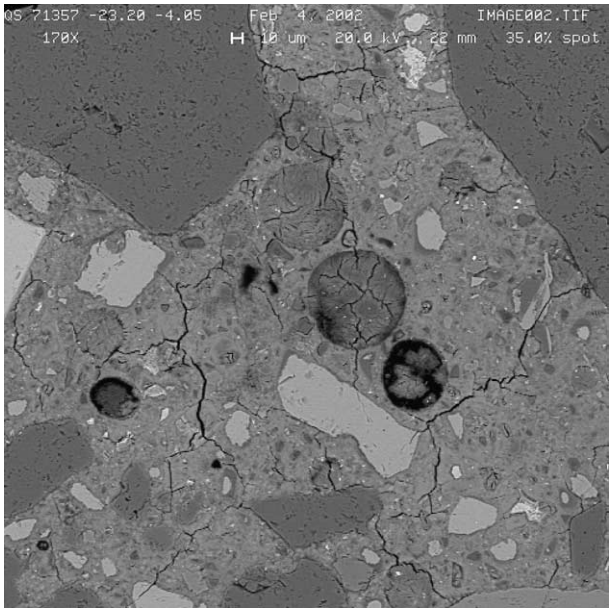

Fig. 2. A network of cracks in the paste, approximately 2 mm below the surface of concrete produced using Type I cement substituted with 45% slag. The crack pattern is typical of that due to sulfate attack.

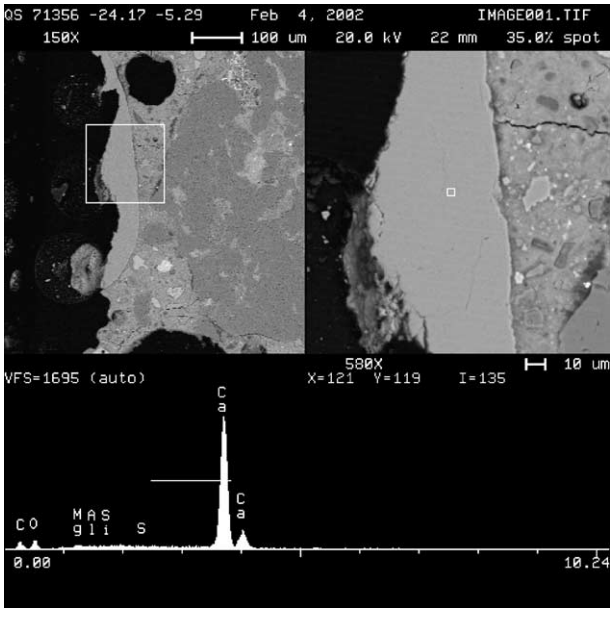

Fig. 1. Dense and featureless carbonated layer, 50–100 μm thick, on the surface of concrete produced using Type I cement substituted with 45% slag.

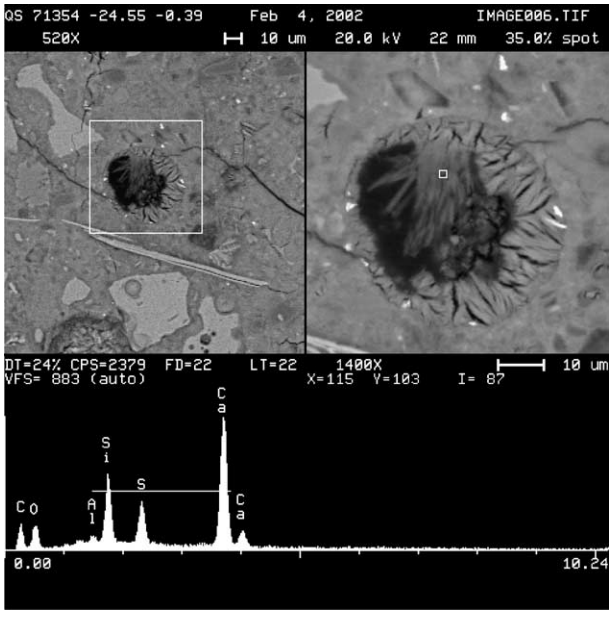

Fig. 3. An air void containing both ettringite and thaumasite. Microstructural differences between the two are evident. The region from which the EDX spectrum was taken is thaumasite.

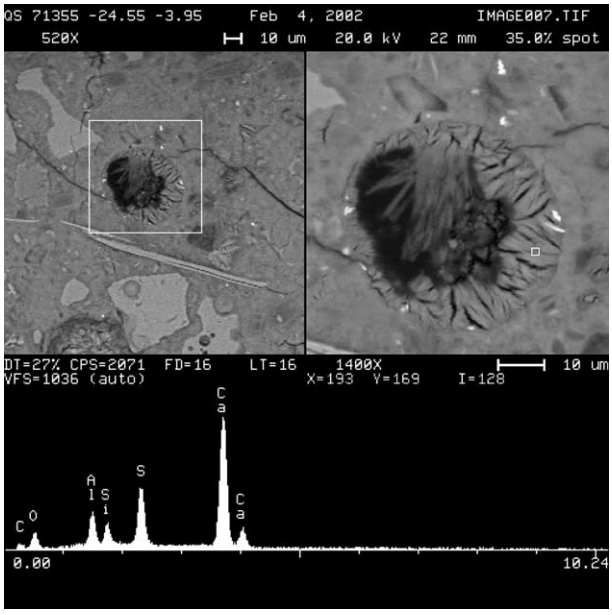

Fig. 4. The same air void as in Fig. 3, but showing the EDX spectrum from the region where ettringite is present.

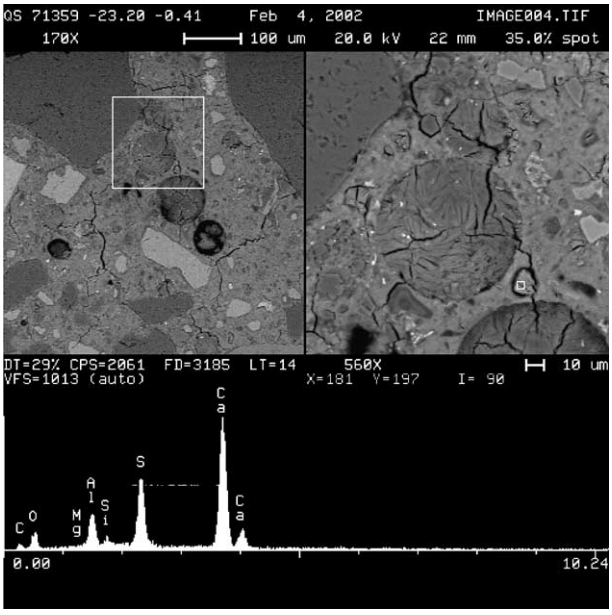

Fig. 6. Paste porosity and air voids filled with ettringite.

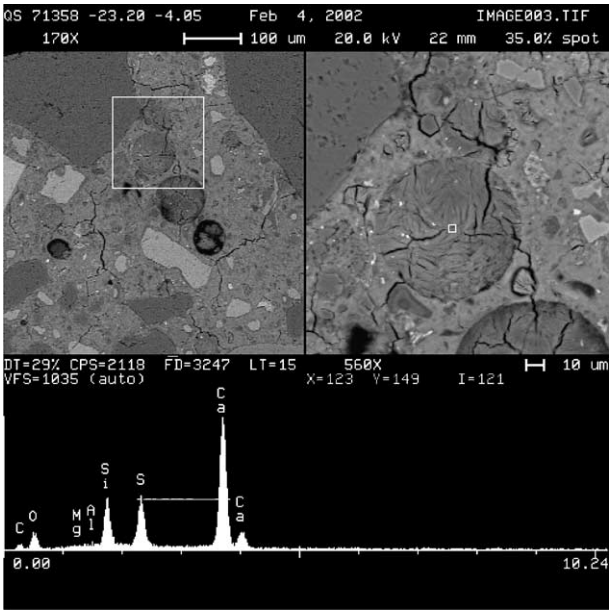

Fig. 5. An air void entirely filled with thaumasite.

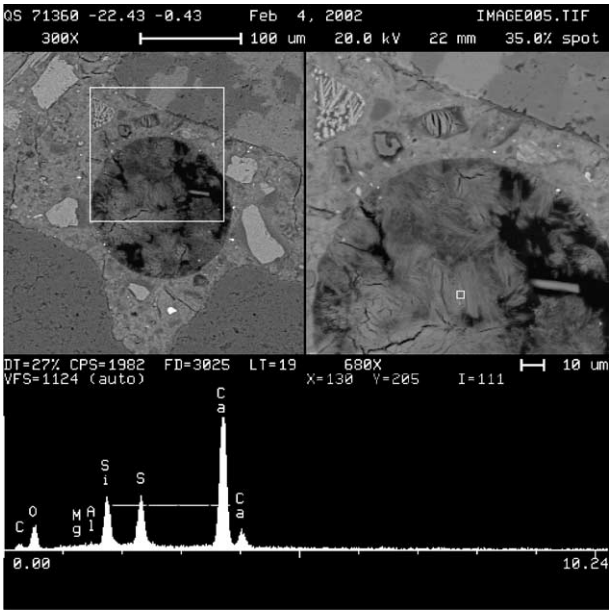

Fig. 7. An air void incompletely filled with thaumasite and an adjacent pore filled with ettringite (immediately above the air void). The EDX spectrum is for the thaumasite.

ettringite. In further support of this hypothesis, Fig. 7 shows an air void partially filled with thaumasite with adjacent paste porosity completely filled by ettringite. These observations are consistent with our hypothesis that ettringite forms first, produces conditions where carbonate intrusion is favored due to crack formation, and then thaumasite forms [6,7].

A variety of air voids show structures indicative of the mechanistic path taken in sulfate transport. Fig. 8 shows the evolution of microstructure across the paste–air void interfacial zone near an aggregate particle. The composition of the cement paste in this zone shows distinct sulfate enrichment. The EDX spectrum in Fig. 8 also indicates the presence of Mg and Al in this paste. This may reflect the hydration of the adjacent slag particle or may merely be the result of interaction volume impinging on this particle. While the comparison is

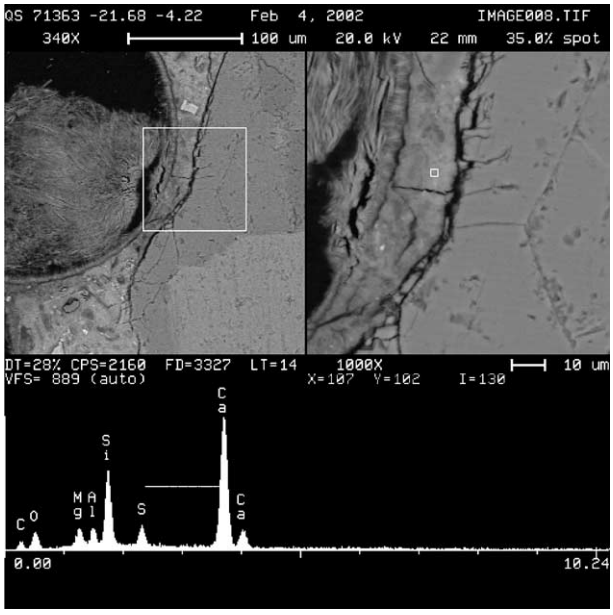

Fig. 8. Microstructural variations across the paste–air void interface region adjacent to an aggregate particle; sulfate accumulation in the paste is evident from its EDX spectrum.

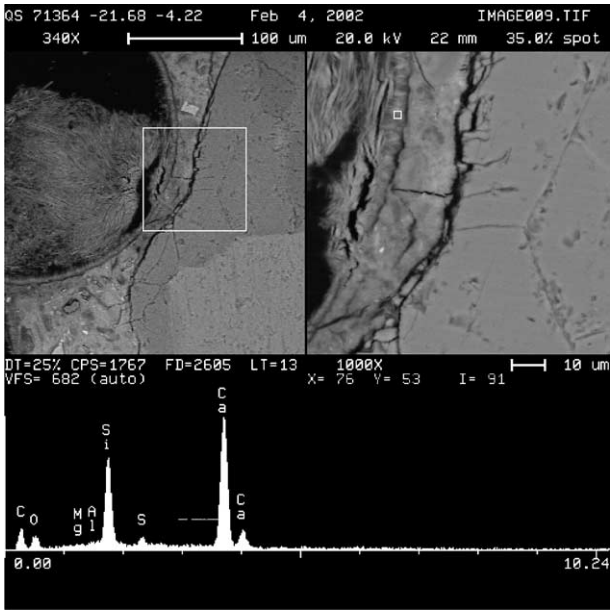

Fig. 9. Compared to that shown in Fig. 8, the sulfate content of the paste in closer proximity to ettringite within the air void is reduced.

qualitative, Fig. 9 shows the paste in close proximity to an ettringite deposit in the air void contains a lower proportion of sulfate. This is consistent with ettringite serving as a sink for sulfate. Fig. 10 shows ettringite in the air void to be in apposition with this paste. Thaumasite is present near the center of the filled void, Fig. 11. The sulfate gradient and the distributions of

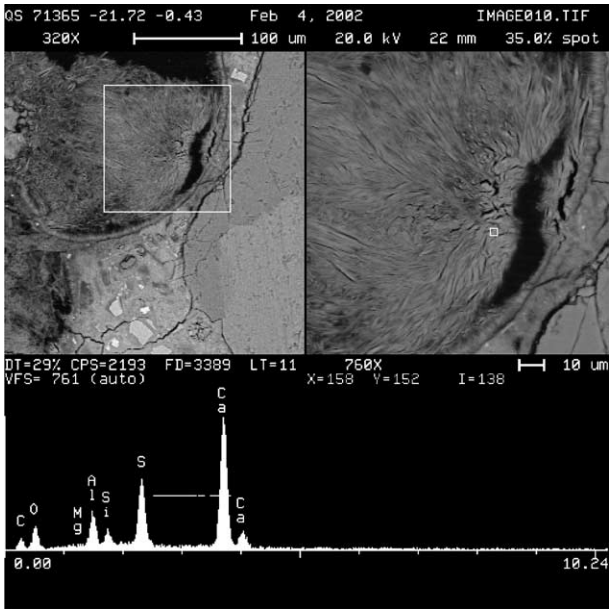

Fig. 10. The presence of ettringite in an air void, consistent with the sulfate gradient in the paste supporting ettringite formation.

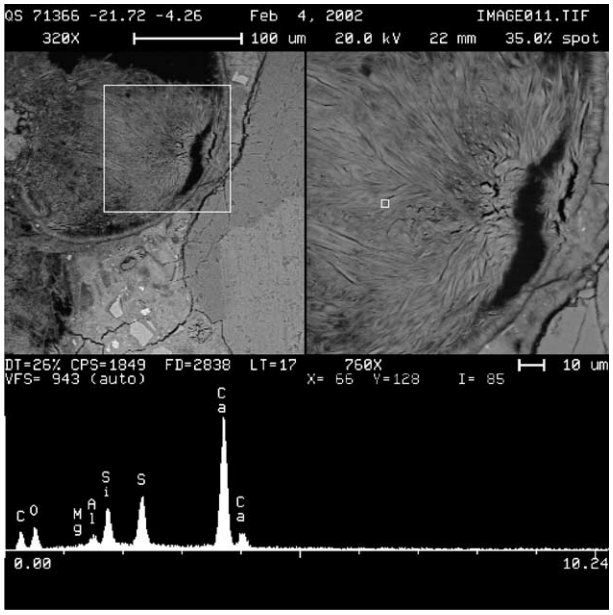

Fig. 11. Thaumasite is present in the center of the air void.

these solids are in accord with the above-described reaction sequence.

The above-described microstructural evolution occurs over a distance of about 5 mm. The transitional region is shown in Fig. 12. The left half of the image area shows filled air voids while the air voids in the right half of the image area are lightly filled. The diminution in paste damage, associated with the reduction in density of cracks from left to right, is evident in the figure.

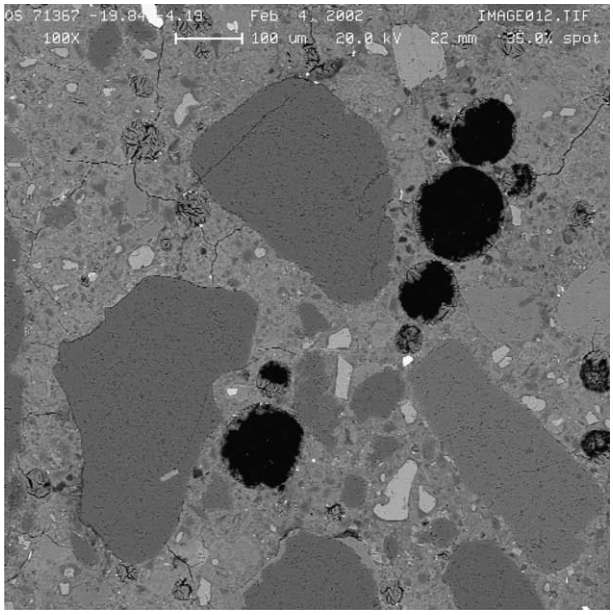

Fig. 12. The transition from a region of paste showing significant damage (on left) to a region showing little damage paste (on right). Incompletely filled air voids are present at the transition.

3.2. Type I cement + 72% slag, w/cm = 0.50 concrete exposed to 50,000 ppm of Na_2SO_4

Microstructures similar to those described above for the binder comprised of Type I cement with 45% slag substitution are also observed when the extent of substitution is 72%. Fig. 13 shows the transition from the carbonate surface layer to a decalcified zone to the distressed paste region. The distressed region, which is about 4 mm in thickness, shows the same features as were described above. The primary microstructural difference observed as a consequence of the increased proportion of slag is the occurrence of the decalcified layer. With the exception of near-surface decalcification at 72% slag substitution, there is little difference between the depths of sulfate attack between the two slag-containing concretes.

3.3. Type II cement, w/cm = 0.50 concrete exposed 50,000 ppm of Na_2SO_4

Microstructural evolution under these experimental conditions has been previously described [7]. Fig. 14 [7] is shown here for comparative purposes and illustrates that the thickness of the carbonated layer to be much greater in the absence of slag, even though the w/cm ratio is constant at 0.5. As Table 1 shows, the depth of sulfate damage is also much greater. These data indicate the benefits of permeability reduction associated with the use of slag.

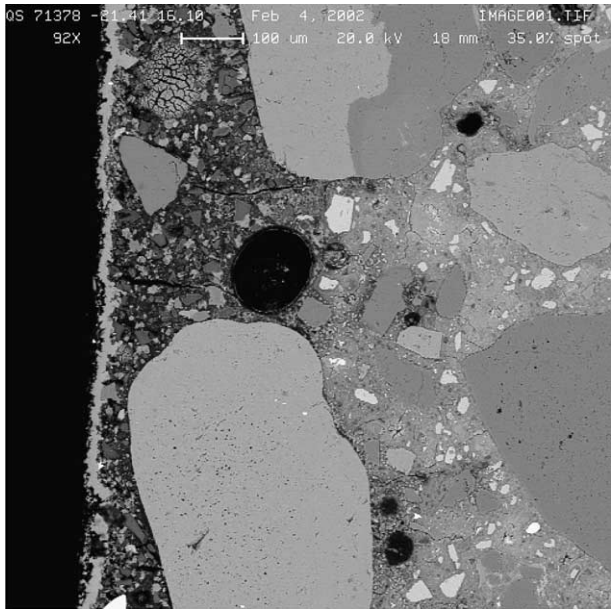

Fig. 13. Microstructural evolution from the surface inwards for concrete produced using Type I cement substituted with 72% slag. A carbonate layer forms the perimeter surface of this concrete. Beneath this is a decalcified zone. Cracks can be seen in the decalcified zone and the paste immediately behind it.

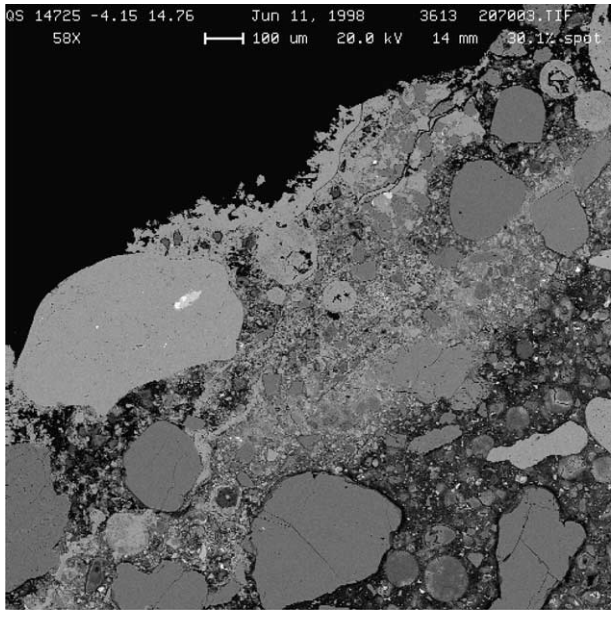

Fig. 14. The carbonated zone that has developed for concrete prepared using Type II cement [1].

3.4. Type V cement, w/cm = 0.45 concrete exposed to 50,000 ppm of Na_2SO_4

Fig. 15 shows a carbonated zone 200–300 μm in thickness. The reduction in w/cm ratio also reduces the extent of carbonate layer formation. This figure also shows that significant deterioration to paste can occur

Table 1
Depth of sulfate attack after long-term exposure to magnesium sulfate or sodium sulfate solutions

Cement type	w/cm Ratio	Attacking species	Duration of exposure (years)	Depth of attack observed (mm)	Reference
V	0.45	$MgSO_4$	21	7	[7]
V	0.45	Na_2SO_4	21	22	[7]
II	0.50	$MgSO_4$	21	32	[7]
II	0.50	Na_2SO_4	21	>37.5	[7]
I + 45% slag	0.50	$MgSO_4$	23	6	[6]
I + 45% slag	0.50	Na_2SO_4	23	5	This study
I + 72% slag	0.50	$MgSO_4$	23	5	[6]
I + 72% slag	0.50	Na_2SO_4	23	4	This study

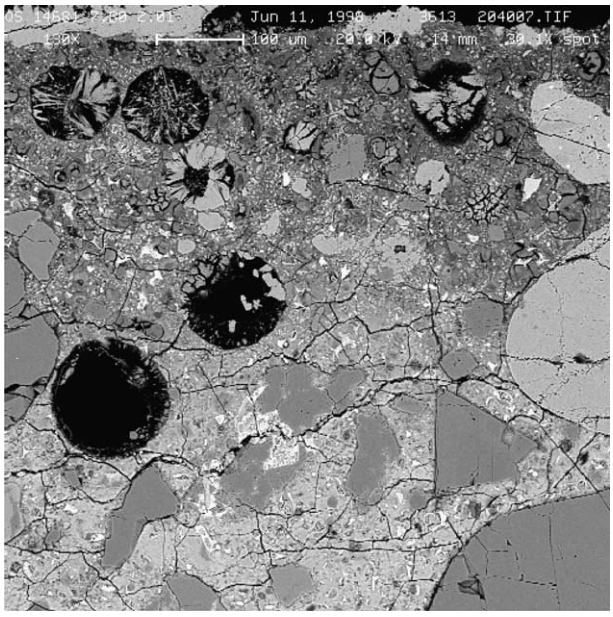

Fig. 15. Microstructural evolution inwards from a perimeter surface (top of micrograph) of concrete prepared using Type V cement. A carbonated zone, a decalcified zone, and a zone of intense paste damage, which overlaps these and extends further inwards, are present.

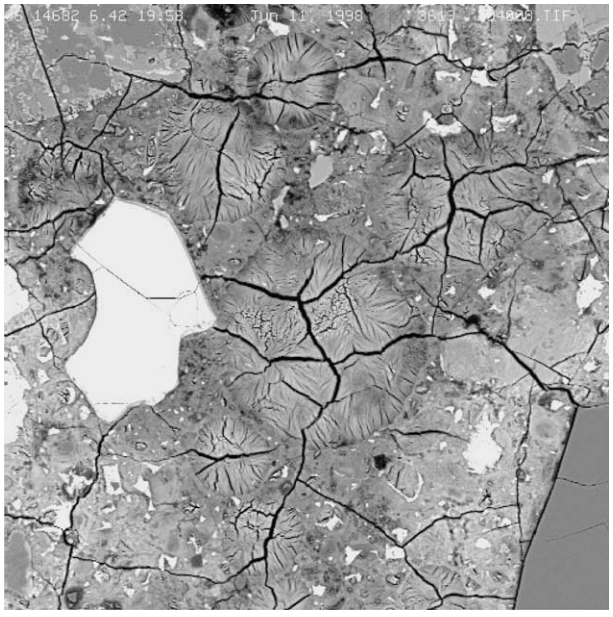

Fig. 16. A region of paste in the Type V concrete in which the air voids are filled. The pattern of cracking appears to be indifferent to these filled voids, passing directly through them.

prior to the filling of the air voids. Cracks caused by expansion also pass through filled voids, Fig. 16.

3.5. Comparison of results

In previous reports we analyzed the spatial evolution of microstructure when the above-described concrete compositions were immersed in 50,000 ppm $MgSO_4$ solution [6,7]. Those observations indicated the absence of significant carbonate layers when concretes were made using Type II or Type V cements. Rather, brucite and/or magnesium silicate layers formed [7]. Table 1 illustrates that the depths of sulfate attack are also reduced when these layers are present. The formation of brucite and/or magnesium silicate layers, however, does not entirely preclude the ingress of carbonate or sulfate because thaumasite and ettringite were generally observed. The driving force for ettringite formation at depth within the concretes can be readily understood in terms of the existence of a concentration gradient driving force due to the exposure to 5% solutions of $MgSO_4$ or Na_2SO_4. The formation of thaumasite at depth in these samples is mechanistically interesting. Thaumasite formation is generally thought to occur when calcium carbonate, C–S–H and sulfate react. Unless the coarse aggregate is serving as the source of carbonate, the present data indicate that thaumasite formation can occur in the absence of an immediately-adjacent carbonate-containing solid precursor. Because thaumasite formation requires a carbonate source, microstructural damage caused by ettringite formation appears to provide a mechanism by which carbonic acid or bicarbonate can become available.

In some instances, the above-described effects are strongly influenced by the presence of blast furnace slag. Table 1 illustrates slag to be highly effective in reducing the depths of sulfate attack, regardless of whether the

associated cation is sodium or magnesium. This generality appears to be associated with the permeability reduction associated with the presence of slag. After 8 years, ASTM C1202 chloride penetration resistance test results were 50, 100, and 5089 Coulombs for the water-stored samples of concretes having w/cm = 0.5 and made with pastes, respectively, containing 72% slag, 45% slag and no slag [5].

The observed depths of attack in concretes containing slag ranged only from about 4 to 6 mm, regardless of the mix design studied and regardless of whether the attacking species was sodium or magnesium sulfate. This, however, may not be true for slags with higher alumina contents.

Elevated sulfate resistance can be attributed to a reduction in permeability. Slag replacement of cement is understood to reduce the rate of diffusion of aggressive ions such as sulfates. Depending on the test procedure employed, McGrath and Hooton [10] found that as little as 25% slag replacement reduced the chloride diffusion coefficients of 0.40 w/cm concretes to between 26% and 40% of those of the control mixtures.

The presence of slag, however, does not significantly reduce the extent of surface carbonate layer formation; no systematic trend was observed regarding carbonate layer formation when these concretes were immersed in water or in sodium sulfate solution, regardless of slag substitution.

4. Conclusions

1. The microstructural evidence supports the hypothesis that ettringite formation precedes that of thaumasite. Associated cracking due to expansion provides a means for ingress of carbon dioxide to support thaumasite formation.
2. When the effects of immersion in magnesium sulfate solution are compared with those of sodium sulfate solution, the deposition of Mg-containing compounds near the surfaces of the concretes studied reduces the depths of attack for concretes produced from Type II or Type V cements.
3. Slag is particularly effective in reducing the extent of sulfate attack regardless of whether by $MgSO_4$ or Na_2SO_4.
4. Over the range studied (45–72%), the proportion of slag was relatively unimportant in conferring sulfate resistance to concrete. The extent of carbonate layer formation is comparable in concretes exposed to water and to 5% sodium sulfate solution.
5. Compared to that in concretes exposed to 5% magnesium sulfate solution and previously reported [1,2], the extent of carbonate layer formation is greater for concretes exposed to 5% sodium sulfate solution.

Acknowledgements

The support of Lafarge for funding the original concrete program is acknowledged along with John Emery of John Emery Geotechnical Engineering Limited for supplying the concrete specimens to the University of Toronto. The microscopy was performed at R.J. Lee Group.

References

[1] Verbeck GJ. Field and laboratory studies of the sulphate resistance of concrete. In: Performance of concrete. Univ. Toronto Press; 1967. p. 113–24.
[2] Khatri RP, Sirivivatnanon V, Yang JL. Role of permeability in sulphate attack. Cement Concrete Res 1997;27(8):1179–89.
[3] Lea F. The chemistry of cement and concrete. Edward Arnold; 1970. p. 338–59.
[4] Gollup RS, Taylor HFW. Microstructural and microanalytical studies of sulfate attack IV. Reactions of a slag cement paste with sodium and magnesium sulfate solutions. Cement Concrete Res 1996;26(7):1013–28.
[5] Gollup RS, Taylor HFW. Microstructural and microanalytical studies of sulfate attack V. Comparison of different slag blends. Cement Concrete Res 1996;26(7):1029–44.
[6] Brown PW, Hooton RD, Clark B. The coexistence of thaumasite and ettringite in concrete exposed to magnesium sulfate at room temperature and the influence of blast-furnace slag substitution on sulfate resistance. Cement Concrete Compos 2003;25(8):939–45.
[7] Brown PW, Hooton RD. Ettringite and thaumasite formation in laboratory concretes prepared using sulfate-resisting cements. Cement Concrete Compos 2002;24:361–70.
[8] Hooton RD, Emery JJ. Sulfate resistance of a Canadian slag cement. ACI Mater J 1990;87(6):547–55.
[9] Brown PW, Skalny JP. Microstructural observations of sulfate attack in field concrete. In: Jany L, Nisperos A, editors. Proceedings of the 24th International Conference on Cement Microscopy, 2002. p. 189–203.
[10] McGrath PF, Hooton RD. Effect of binder composition on chloride penetration resistance of concrete. In: Proceedings of the Fourth International Conference on Durability of Concrete, Sydney, ACI SP-170, vol. 1, 1997. p. 331–47.